

Competition and coexistence of antiferromagnetism and superconductivity in $R\text{Ba}_2\text{Cu}_3\text{O}_{6+x}$ ($R = \text{Lu}, \text{Y}$) single crystals

A. N. Lavrov,¹ L. P. Kozeeva,¹ M. R. Trunin,² and V. N. Zverev²

¹*Institute of Inorganic Chemistry, Lavrentyeva-3, Novosibirsk 630090, Russia*

²*Institute of Solid State Physics, Institutskaya-2, Chernogolovka 142432, Moscow region, Russia*

(Dated: November 11, 2018)

We use c -axis resistivity and magnetoresistance measurements to study the interplay between antiferromagnetic (AF) and superconducting (SC) ordering in underdoped $R\text{Ba}_2\text{Cu}_3\text{O}_{6+x}$ ($R = \text{Lu}, \text{Y}$) single crystals. Both orders are found to emerge from an anisotropic 3D metallic state, upon which antiferromagnetism opposes superconductivity by driving the doped holes towards localization. Despite the competition, the superconductivity sets in before the AF order is completely destroyed and coexists with latter in a certain range of hole doping. We find also that strong magnetic fields affect the AF-SC interplay by both suppressing the superconductivity and stabilizing the Néel order.

PACS numbers: 74.25.Fy, 74.25.Dw, 75.30.Kz, 75.47.-m, 74.72.Bk

I. INTRODUCTION

In high- T_c cuprates, the conducting state develops gradually as the parent antiferromagnetic (AF) insulator is doped with charge carriers.^{1,2,3} At a certain point of this transformation the superconductivity (SC) sets in, which happens long before such remnants of the AF insulating state as AF correlations and a pseudogap in the electron density of states are completely wiped out.^{1,2,3,4} Despite the decades of intensive research, however, detail mechanisms of the insulator-metal transformation and, in particular, the role of AF correlations therein remain unclear. From the experimental point of view, the difficulty stems from the very strong exchange interaction in CuO_2 planes, $J \sim 0.1 \text{ eV}$,^{1,4} which makes the AF correlations robust to high temperatures and magnetic fields and leaves no means of “switching” them off. For compositions on either side of the insulator-superconductor transformation, two-dimensional (2D) AF correlations nucleate in CuO_2 planes already at high temperatures $T \sim J/k_B$. As the temperature decreases, the spin correlations smoothly develop until—depending on the doping level—establishing a long-range AF order at the Néel temperature T_N , forming a static or fluctuating “stripe” structure, or freezing into a “cluster spin glass”.^{1,4,5,6,7} This evolution being spread over a wide temperature range makes it hard to clarify whether and how the spin textures emerging in CuO_2 planes affect the charge motion.

In contrast to the gradual development of 2D AF correlations within the CuO_2 planes, the spin ordering along the c axis—if it takes place at all—occurs in a dramatically compressed temperature interval. Owing to the strong anisotropy of exchange interactions, the c -axis spin correlation length ξ_c^{AF} stays shorter than the interplane distance until the 3D ordering temperature T_N is closely approached.^{1,4} Only in the vicinity of T_N , ξ_c^{AF} reaches the unit-cell size, causing a 2D–3D crossover in AF correlations, and then diverges sharply. In fact, it is this abrupt spin ordering along the c direction that allows

the AF transition to show up in macroscopic properties of lightly doped cuprates. In $R\text{Ba}_2\text{Cu}_3\text{O}_{6+x}$ crystals (R is a rare earth element), for instance, the c -axis resistivity $\rho_c(T)$ exhibits a steep increase below T_N , though $\rho_{ab}(T)$ stays perfectly smooth through T_N .^{8,9,10} Hence, although AF correlations within CuO_2 planes are hard to affect, the abrupt AF ordering along the c axis opens a possibility to compare the electron transport *with* and completely *without* spin order along one of the directions, thus clarifying the transport mechanisms and the interplay between magnetism and superconductivity.

In this paper, we report a c -axis magnetoresistance (MR) study of $\text{LuBa}_2\text{Cu}_3\text{O}_{6+x}$ (Lu-123) and $\text{YBa}_2\text{Cu}_3\text{O}_{6+x}$ (Y-123) single crystals with doping levels spanning the range of the AF-SC transformation. Sharp AF transitions observed in crystals even with low $T_N \approx 20 \text{ K}$ have allowed us to map precisely the phase diagram and to single out the impact of spin ordering on the c -axis charge transport. We find that in the doping region of the AF-SC transformation the (Lu,Y)-123 crystals exhibit a 3D metallic conduction until the SC or AF ordering intervenes at low temperatures. The Néel ordering appears to compete with SC by strongly inhibiting the charge motion, yet nevertheless the two orders coexist in a certain range of hole doping. Interestingly, the magnetic field is found to interfere with both orders, suppressing the superconductivity and stabilizing the static AF order.

II. EXPERIMENTAL DETAILS

$R\text{Ba}_2\text{Cu}_3\text{O}_{6+x}$ single crystals with non-magnetic rare-earth elements $R = \text{Lu}$ and Y were grown by the flux method and their oxygen stoichiometry was tuned to the required level by subsequent high-temperature annealing and quenching.^{8,11} Given the complex distribution of structural defects along the c axis in flux-grown crystals,¹¹ part of the crystals were cut and polished to select better pieces for measurements. We confirmed also

that no oxygen-enriched layer was formed at the crystal surface upon quenching; namely, one of the crystals was dissolved in acid in several steps, each step being preceded with resistivity measurements, yet no considerable change in the SC transition was observed.

After the doping level of $R\text{Ba}_2\text{Cu}_3\text{O}_{6+x}$ crystals was roughly set by changing the oxygen content x , the hole density in CuO_2 planes n_h was further reversibly tuned using the well studied phenomenon of chain-layer oxygen ordering: heating the crystal above 100-120°C with subsequent quenching reduced the hole density in CuO_2 planes by up to 20%, while room-temperature aging gradually restored it back without any change in stoichiometry.^{8,9} For characterizing the doping state of crystals we have selected the in-plane conductivity $\sigma_{ab}(280\text{ K})$. The latter is a good measure of the hole density given that the hole mobility stays almost constant in the doping region under investigation.² The particular temperature $T = 280\text{ K}$ is taken to be high enough to reduce the impact of impurity scattering, yet sufficiently low to avoid oxygen ordering, and thus change in doping, on the time scale of measurements. It is worth noting that although the in-plane and the c -axis transport measurements were carried out on separate samples, the samples were cut from the same crystal, and then annealed and handled together to provide an exact match in their states.

The c -axis resistivity $\rho_c(T)$ was measured using the ac four-probe technique with a special care taken to avoid mixing of ρ_c with the in-plane resistivity ρ_{ab} . To provide a homogeneous current flow along the c -axis, two current contacts were painted to almost completely cover the opposing ab -faces of the crystal, while two voltage contacts were placed in small windows reserved in the current ones.^{8,9,10} Magnetoresistance measurements were carried out either by sweeping temperature at fixed magnetic fields $\mathbf{H} \parallel \mathbf{c}$ up to 16.5 T or by sweeping the field at fixed temperature.

III. RESULTS

A. n_h - T - H phase diagram

In $R\text{Ba}_2\text{Cu}_3\text{O}_{6+x}$, the hole density in CuO_2 planes, n_h , can be tuned continuously by changing the degree of oxygen ordering (see Sec. II). This provides a number of states with different n_h for a given oxygen content x , thereby allowing critical regions of the phase diagram to be studied in detail. We have used this approach to trace how the c -axis resistivity of $\text{LuBa}_2\text{Cu}_3\text{O}_{6+x}$ single crystals evolves with the hole density in the narrow doping region where superconductivity sets in (Fig. 1). As can be seen, the $\rho_c(T)$ curves in this heavily underdoped region demonstrate a complicated behavior with a crossover¹² at 100-150 K. At temperatures above the crossover, the c -axis resistivity smoothly decreases with increasing hole density, and no peculiarity shows up in this smooth evo-

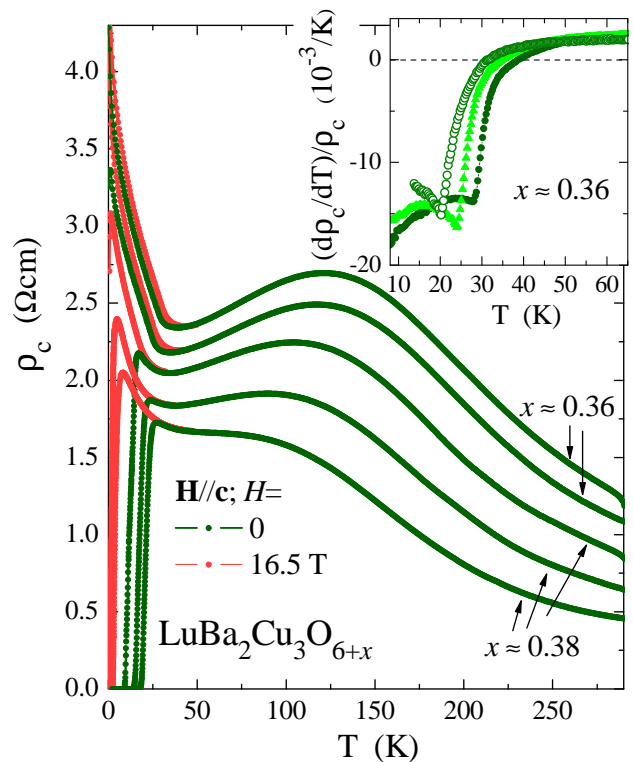


FIG. 1: (Color online) Out-of-plane resistivity, $\rho_c(T)$, of a $\text{LuBa}_2\text{Cu}_3\text{O}_{6+x}$ single crystal at several hole-doping levels near the AF-SC transformation; the hole doping was tuned by changing the oxygen content x and the degree of oxygen ordering (several states for each x). The data were taken at zero and 16.5-T magnetic field applied along the c axis. Inset: An anomaly in the normalized derivative $(d\rho_c/dT)/\rho_c$ associated with the Néel transition; measurements were done after quenching the crystal (\bullet) as well as after room-temperature aging for several hours (\blacktriangle) and days (\circ).

lution at the doping level of the SC onset. The low- T resistivity behavior, however, changes remarkably. From the set of zero-field $\rho_c(T)$ curves in Fig. 1 one can immediately infer that, upon cooling, the crystal either turns into the SC state, or instead exhibits a steep increase in the resistivity. This steep growth in $\rho_c(T)$ with a characteristic asymmetric negative peak in the derivative (inset in Fig. 1) is a hallmark of the Néel transition in $R\text{Ba}_2\text{Cu}_3\text{O}_{6+x}$.^{8,9,10} The evolution of $\rho_c(T)$ curves looks therefore like AF and SC are competing for carriers and the system falls into one of two possible states, either the insulating AF state or the SC one. It is worth emphasizing that sharp AF transitions are observed down to remarkably low $T_N \approx 20\text{ K}$ (inset in Fig. 1) instead of the freezing into a spin glass usually expected at such temperatures⁵; the superconductivity in Lu-123 thus develops directly from the AF state without any intervening spin-glass region.

One may wonder whether a strong magnetic field will suppress both the AF and SC orders and create some intermediate metallic state. We find, surprisingly, that

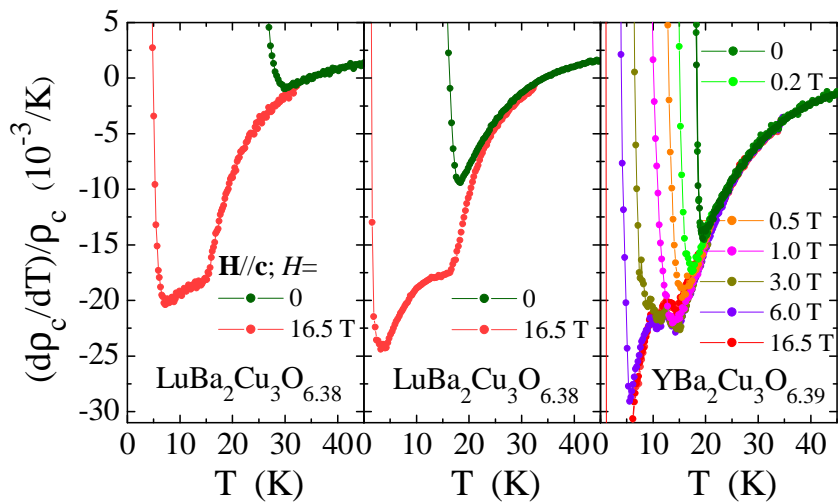


FIG. 2: (Color online) Suppression of the superconductivity with the magnetic field in Lu-123 and Y-123 crystals. The unveiled normal-state resistivity exhibits an anomaly associated with the Néel transition (compare with the inset in Fig.1).

upon suppressing the superconductivity the field $\mathbf{H} \parallel \mathbf{c}$ also recovers the steep increase in ρ_c associated with the AF ordering (Fig. 1). A study of other crystals has confirmed that as long as the SC is weak enough to be wiped out with the 16.5-T field, be that in Lu-123 or Y-123 crystals, the obtained normal-state $\rho_c(T)$ curves demonstrate clear anomalies at 15-20 K associated with the Néel transition (Fig. 2). This behavior indicates that either the AF and SC orders coexist and the magnetic field simply unveils the resistivity anomaly at T_N hidden by superconductivity, or the AF order is frustrated in the SC state but revives as the superconductivity is destroyed.

Although the Néel transitions in Figs. 1 and 2 look rather sharp for transition temperatures reduced by 20-25 times from the original $T_{N0} \approx 410-420$ K in parent $R\text{Ba}_2\text{Cu}_3\text{O}_6$,⁴ their width together with insufficient understanding of the interlayer charge transport still introduce a considerable uncertainty in the T_N evaluation. Indeed, depending on the mechanisms underlying the observed c -axis resistivity anomalies, T_N should be taken at the position of the negative peak in the derivative $d\rho_c/dT$ or at the middle of the “drop” in $d\rho_c/dT$ preceding the peak. These two definitions provide T_N values that differ by several K for the curves shown in Figs. 1 and 2. Nevertheless, whichever approach in evaluating T_N is selected, the qualitative conclusion on the long-range AF order with $T_N \approx 15-20$ K showing up in low- T_c samples (Fig. 2) remains unchanged.

The phase diagram in Fig. 3 presenting T_c and T_N as a function of the in-plane conductivity $\sigma_{ab}(280K)$ (see Sec. II) makes the overlap of the AF and SC regions in $R\text{Ba}_2\text{Cu}_3\text{O}_{6+x}$ apparent. The main panel in Fig. 3 depicts a general view of the AF-SC transformation established for several crystals systematically driven through the entire doping range (most data are taken from our previous studies^{8,9}), while the enlarged view of the critical region with new data points is shown in the inset. As

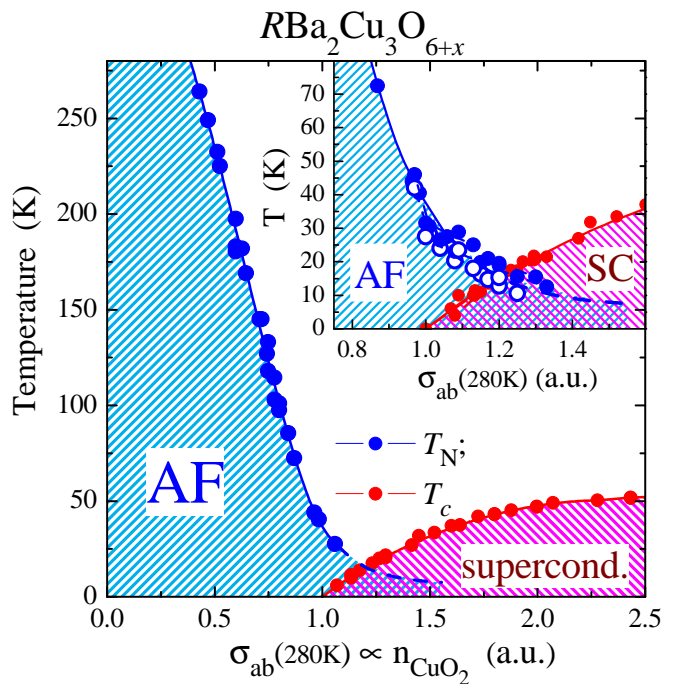


FIG. 3: (Color online) A phase diagram of $R\text{Ba}_2\text{Cu}_3\text{O}_{6+x}$ ($R = \text{Lu, Tm, Y}$) crystals presenting the AF and SC transition temperatures, T_N and T_c , as a function of the in-plane conductivity $\sigma_{ab}(280K)$ that is roughly proportional to the hole density. (To avoid uncertainty associated with the samples’ geometry, $\sigma_{ab}(280K)$ was normalized by its value at the SC onset). The critical region of the phase diagram is shown in the inset. The Néel temperature was determined either by the position of the negative peak in the derivative $d\rho_c/dT$ (open circles), or at the middle of the drop in the derivative (solid circles). Note that in SC samples the T_N values were determined after suppressing the superconductivity with 16.5-T field $\mathbf{H} \parallel \mathbf{c}$.

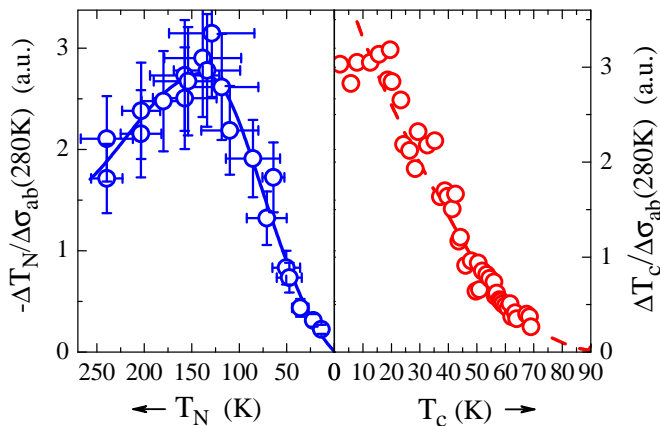


FIG. 4: (Color online) Shifts of T_N and T_c normalized by corresponding changes in σ_{ab} as observed upon room-temperature aging of $R\text{Ba}_2\text{Cu}_3\text{O}_{6+x}$ crystals. The data are presented as a function of T_N and T_c . The horizontal bars in the left panel indicate the actual interval of the T_N shift in each experiment.

can be seen, the AF phase boundary does not terminate at the onset of superconductivity. Instead, it extends at least up to 30% higher doping, and crosses the T_c line at ≈ 15 K, in contrast to another prototype high- T_c cuprate $\text{La}_{2-x}\text{Sr}_x\text{CuO}_4$ where the long-range AF order is destroyed long before the SC sets in.^{1,5}

An important issue is the reliability of the presented phase diagram, especially given the controversy remaining in publications.^{4,5,13,14} Indeed, the observed SC and AF transitions are not very sharp, leaving some room for doubts. Besides, however sharp the transitions might be, a possibility of a peculiar macroscopic inhomogeneity imitating the phase coexistence will still remain. For the oxygen compositions under discussion, we have ruled out one possible source of inhomogeneity associated with a phase separation into oxygen-rich and oxygen-poor domains: The behavior of Lu-123 crystals quenched from high temperatures, and thus possessing homogeneous oxygen distribution, showed no qualitative difference from that of crystals aged at room temperature for an ultimate 10-years period.

A static cation inhomogeneity over the crystal as a source of the AF and SC phase coexistence is, however, hard to rule out by conventional means. Fortunately, in R-123 crystals one has an additional tool to check the phase diagram by employing the hole doping through the oxygen ordering.^{8,9} In fact, by aging the crystals at room temperature and measuring their conductivity $\sigma_{ab}(280\text{K})$, T_c , and T_N as a function of time, one can evaluate the slopes of phase boundaries in the diagram shown in Fig. 3. An important point here is that the relative changes in T_c and T_N observed upon aging are insensitive to static macroscopic inhomogeneities. The phase-boundary slopes measured in the described way are presented in Fig. 4 as a function of T_c and T_N ; this way of the data presentation is selected to avoid any uncer-

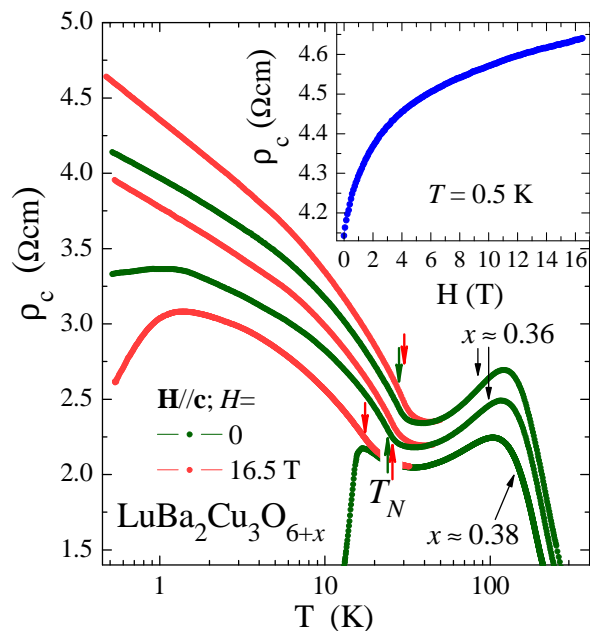


FIG. 5: (Color online) Semilogarithmic plot of $\rho_c(T)$ illustrating the additional low- T resistivity caused by the AF ordering and the impact of the magnetic field $\mathbf{H} \parallel \mathbf{c}$ on both T_N and ρ_c . Two sets of curves for $x \approx 0.36$ correspond to the quenched and partially aged states of the crystal. Low- T magnetoresistance data for the quenched $x \approx 0.36$ sample are shown in the inset.

tainty related to ill-defined parameters such as the hole density. As expected, the slope of the SC phase boundary, $\Delta T_c / \Delta \sigma_{ab}(280\text{K})$, gradually increases with decreasing T_c and the superconductivity disappears abruptly at a critical doping. The behavior of the AF boundary is much different; initially it indeed becomes steeper with increasing doping and decreasing T_N , but then the slope of the T_N line decreases dramatically, tending to zero at zero T_N . This flattening unambiguously confirms the intrinsic origin of the AF-order tail entering the SC region in the phase diagram in Fig. 3.

What still remains to be clarified is whether the AF and SC orders actually coexist in their overlapping region on the phase diagram, or the AF order is restored by the magnetic field upon destroying the superconductivity. The latter is not completely impossible given that the magnetic field is found to inhibit the hole motion and to stabilize the Néel order even in non-SC $R\text{Ba}_2\text{Cu}_3\text{O}_{6+x}$ crystals (Fig. 5). One can see that the Néel temperature indicated in the plot by an arrow, increases by ~ 2 - 3 K under 16.5-T field $\mathbf{H} \parallel \mathbf{c}$. As a result, the corresponding resistivity upturn also starts from higher temperatures, which causes a significant magnetoresistance $\Delta \rho_c / \rho_c$ reaching $\approx 12\%$ at low T (inset in Fig. 5). It is worth recalling that the resistivity measurements are incapable of providing information on T_N values within the SC state and the data points in Fig. 3 located inside the SC region were obtained after the SC was killed by

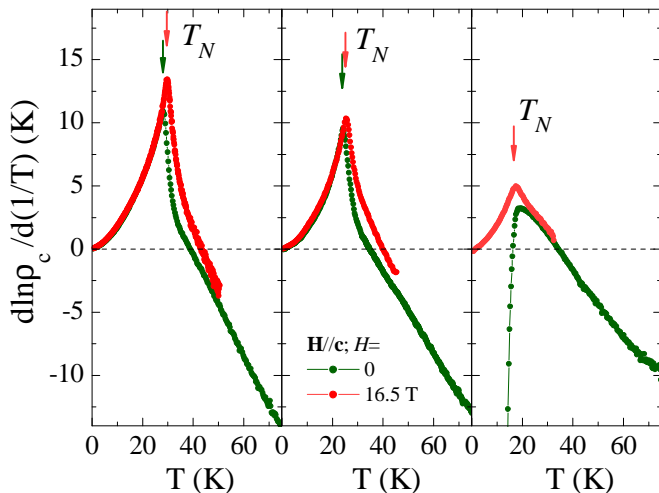


FIG. 6: (Color online) Evolution of the derivative $d \ln \rho_c / d(1/T)$ upon changing the Néel temperature. The data were obtained on the same $\text{LuBa}_2\text{Cu}_3\text{O}_{6+x}$ crystal at $x \approx 0.36$, in the quenched (left panel) and partially aged (middle panel) states, and at $x \approx 0.38$ in the quenched state (right panel).

the 16.5-T magnetic field. If the field-induced increase of T_N in the SC region is two-three times larger than in non-SC ones, the true magnetic state underlying the superconductivity in R -123 may well be a “cluster spin glass” which is driven to a long-range AF order only with the SC suppression.

B. AF order and the c -axis conductivity

After establishing the phase diagram, we can consider what is the “normal state” (at $T > T_N, T_c$) that both the AF and SC orders originate from, and how it is affected by the AF ordering. At a first glance, the long-range antiferromagnetism just localizes the doped holes, thus strictly opposing the superconductivity (Figs. 1 and 5). However, there exists a narrow doping range on the phase diagram in Fig. 3 where the superconductivity sets in at $T < T_N$ (see also Figs. 1 and 2), which raises additional questions concerning the mechanism of hole transport in the AF state. In particular, does the c -axis transport actually acquire an activated character with establishing the long-range AF order? If the AF-ordered state is inevitably an insulator with an appreciable energy gap, how does the superconductivity emerge at $T_c < T_N$?

The simplest way of evaluating the activation energy is to plot the derivative $d \ln \rho_c / d(1/T) = \Delta(T)$ which gives a T -independent Δ for ordinary activation behavior $\rho = A \exp(\Delta/T)$ or an effective gap $\Delta(T) \propto T^{1-k}$ for variable range hopping $\rho = A \exp(B/T^k)$. In contrast to expectations, the derivative data in Fig. 6 show a clear positive curvature ($k < 0$) in the entire temperature region below T_N , which is inconsistent with a simple activated transport. The AF ordering therefore inhibits

the hole motion, causing a sharp kink at T_N , but does not immediately turn the system into an insulator. With further reduction of the carrier density and increase of T_N above 50-100 K, the hole motion indeed switches to the hopping regime,¹⁰ yet in the low- T_N region shown in Figs. 5 and 6 the quasi-metallic conduction survives, leaving some room for superconductivity. Strictly speaking, a possibility that the resistivity even in low- T_N crystals in Figs. 5 and 6 will acquire an insulating behavior in the sub-Kelvin region still remains, but the corresponding insulating gap in that case would be too small to affect the occurrence of superconductivity.

The derivative plots in Fig. 6 have other important implications. First, all the derivatives $d \ln \rho_c / d(1/T)$ at low T appear to follow roughly the same curve until breaking down at T_N . The same low- T resistivity behavior is observed even in superconducting crystals after suppressing SC with magnetic field (right panel). The c -axis transport mechanism in the spin ordered state is therefore kept unchanged in the critical doping range of the AF-SC transformation; what changes with doping and magnetic field is merely the Néel temperature (Fig. 6). Second, the $\rho_c(T)$ upturn at low T —marked by the positive sign of the derivative in Fig. 6—is solely, or at least predominantly caused by the AF ordering. As the spin order melts above T_N , the resistivity quickly switches to the metallic behavior [negative sign of $d \ln \rho_c / d(1/T)$]. With decreasing T_N the region of the resistivity upturn shrinks with a clear tendency to vanish completely for $T_N \rightarrow 0$ (Fig. 6). Therefore, in the $T_N = 0$ limit (if it could be reached without getting into the SC state) the c -axis resistivity would keep the metal-like behavior down to low T , slowly decreasing and approaching a constant value at zero temperature.

The obtained data indicate that, in the absence of the interplane AF order, the charge carriers in $R\text{Ba}_2\text{Cu}_3\text{O}_{6+x}$ can move along the c axis without thermal activation. Regardless of whether the non-activated interlayer conduction occurs through a coherent, metallic transport or by an energy-conserving tunneling, it requires itinerant quasiparticles to be already formed in CuO_2 planes. The latter in turn implies the in-plane charge transport in the non-AF-ordered state to be invariably metallic as well. Indeed, the in-plane resistivity $\rho_{ab}(T)$ was reported to exhibit a metallic behavior without any upturn until entering the Néel state.^{8,9,15} Consequently, the “normal state” playing a role of a starting point for the AF-SC phase competition in $R\text{Ba}_2\text{Cu}_3\text{O}_{6+x}$ is an anisotropic 3D metal that experiences the impact of SC and AF ordering upon lowering the temperature.

IV. DISCUSSION

By now, many theoretical approaches have been suggested to describe the frustration that the doped holes introduce to the spin system and the resulting suppression of the long-range AF order.^{7,16,17,18,19,20,21} Namely,

the doped holes were proposed to switch the exchange interaction between the nearest Cu spins from antiferroto ferromagnetic while being localized,¹⁶ or to continuously break the AF bonds while moving by the nearest-neighbor hopping.^{7,17} Spin distortions accompanying the doped holes are not restricted to the nearest Cu ions, but spread for several unit cells away and may form spin polarons, 2D spin vortices,¹⁸ spin spirals,^{19,20} AF domain walls,⁷ or complex spin textures controlled by the distribution of the dopants.²¹ Whatever the case, upon increasing the hole density, the resulting spin distortions are suggested to gradually reduce the average staggered magnetization in each CuO_2 plane to zero, thereby making impossible the interlayer spin ordering and hence the long-range AF order.

While the mentioned above theoretical approaches have been positively tested on the prototype high- T_c cuprate $\text{La}_{2-x}\text{Sr}_x\text{CuO}_4$, the considerably different behavior of $\text{RBa}_2\text{Cu}_3\text{O}_{6+x}$ may call for reconsidering the impact of doped holes on the long-range AF order. Indeed, the AF state in $\text{RBa}_2\text{Cu}_3\text{O}_{6+x}$ survives up to 2-3 times higher hole concentrations than in $\text{La}_{2-x}\text{Sr}_x\text{CuO}_4$, pointing to a significant material dependence of the AF-order suppression. Furthermore, the low- T_N tail of the AF order spreading in the phase diagram towards SC compositions (Fig. 3) is hard to explain in the framework of those approaches, since they predict no slowing down of the spin frustration with increasing doping. One more difficulty for the existing models is the sharp AF transitions observed down to low T_N 's, which are hard to reconcile with strongly frustrated spin states and disordered spin textures in CuO_2 planes suggested to emerge with doping.^{16,18,21}

Nevertheless, most of the observed features may be qualitatively accounted for by assuming the doped holes to break the long-range AF order in CuO_2 planes into 2D domains.⁷ Indeed, since the Néel temperature in that case should be determined by the interlayer spin coupling integrated over an average domain,^{1,4} a gradual reduction of the domain size with doping can explain why T_N approaches zero value slowly and smoothly instead of vanishing abruptly (Fig. 3). It is worth recalling that the interlayer coupling in $\text{RBa}_2\text{Cu}_3\text{O}_{6+x}$ is not frustrated⁴ in contrast to $\text{La}_{2-x}\text{Sr}_x\text{CuO}_4$,¹ and thus should allow the Néel order in the former to survive up to much higher doping.

The idea of moving holes frustrating the AF order implies a reverse impact as well, which makes the origin of the observed antiferromagnetism-induced hole localization intuitively clear. As the penalty for frustrating the AF bonds exceeds the kinetic energy of a doped hole, the hole should get trapped by the environment. While in CuO_2 planes the hole hopping to the nearest-neighbor sites is inhibited smoothly² due to the gradual development of AF correlations, the suppression of the c -axis hole hopping should occur abruptly with the c -axis spin ordering at T_N , exactly as observed experimentally. However a question remains: when exactly does

the charge transport switch its character from metallic to non-metallic, i.e. thermally-activated hopping? A comparison of the c -axis conductivity for the cases of spins being or being not AF ordered along that axis has demonstrated that in the absence of spin order the holes move without thermal activation. Therefore, the “normal state” in the AF-SC transformation region (at temperatures above T_N , T_c) is certainly a 3D metal. As the AF order develops, the holes are driven to localization, yet the exact position of the metal-insulator transition (MIT) remains unsettled.

Previous attempts to determine the MIT location on the phase diagram of $\text{RBa}_2\text{Cu}_3\text{O}_{6+x}$ employed both the charge-transport and heat-transport measurements, yet resulted in somewhat controversial conclusions; namely, the MIT was suggested to occur at hole densities lower, equal, or even higher than the SC onset (see Refs. 22,23 and references therein). Is there a universal doping level for MIT in $\text{RBa}_2\text{Cu}_3\text{O}_{6+x}$ at all? An important result following from the present study is that the metal-insulator transformation is largely driven by the AF spin ordering. Given that the AF correlations in $\text{RBa}_2\text{Cu}_3\text{O}_{6+x}$ are not determined solely by the hole density, but develop with decreasing temperature, get stabilized by magnetic fields and, presumably, depend on some material parameters, there is little reason to expect the MIT to be located on the phase diagram at some universal hole density. Instead, the metal-insulator transformation may take place depending on doping, magnetic field, material parameters, and, in a sense, even on temperature. The latter means that the hole localization gains strength on cooling due to the development of the AF order and thus the metal-insulator border may be crossed at some transition temperature.²⁴

What still remains to be understood is how the magnetic field enters the AF-SC interplay. One possibility is that the magnetic field affects both orders almost independently, suppressing superconductivity and stabilizing the long-range AF state. Indeed, a magnetic field applied to a 2D Heisenberg antiferromagnet can introduce an anisotropy to the spin system, thus suppressing the spin fluctuations and allowing the long-range Néel order to be established. Alternatively, the AF and SC ground states may be separated by a first-order transition, as were predicted, for instance, in the $\text{SO}(5)$ theory,²⁵ and the magnetic field may directly affect their competition. Microscopic probes capable of detecting the AF order inside the superconducting state are indispensable for this issue to be clarified.

Acknowledgments

We thank V. F. Gantmakher and D. V. Shovkun for fruitful discussions and acknowledge support by RFBR (grants 05-02-16973 and 09-02-01224) and the integration project SB RAS No.81.

-
- ¹ M. A. Kastner, R. J. Birgeneau, G. Shirane, and Y. Endoh, *Rev. Mod. Phys.* **70**, 897 (1998).
- ² Y. Ando, A. N. Lavrov, S. Komiyama, K. Segawa, and X. F. Sun, *Phys. Rev. Lett.* **87**, 017001 (2001).
- ³ T. Yoshida, X. J. Zhou, T. Sasagawa, W. L. Yang, P. V. Bogdanov, A. Lanzara, Z. Hussain, T. Mizokawa, A. Fujimori, H. Eisaki, Z.-X. Shen, T. Kakeshita, and S. Uchida, *Phys. Rev. Lett.* **91**, 027001 (2003).
- ⁴ J. M. Tranquada, A. H. Moudden, A. I. Goldman, P. Zolliker, D. E. Cox, G. Shirane, S. K. Sinha, D. Vaknin, D. C. Johnston, M. S. Alvarez, A. J. Jacobson, J. T. Lewandowski, and J. M. Newsam, *Phys. Rev. B* **38**, 2477 (1988).
- ⁵ Ch. Niedermayer, C. Bernhard, T. Blasius, A. Golnik, A. Moodenbaugh, and J. I. Budnick, *Phys. Rev. Lett.* **80**, 3843 (1998).
- ⁶ J. M. Tranquada, B. J. Sternlieb, J. D. Axe, Y. Nakamura, and S. Uchida, *Nature* **375**, 561 (1995).
- ⁷ S. A. Kivelson, I. P. Bindloss, E. Fradkin, V. Oganesyan, J. M. Tranquada, A. Kapitulnik, and C. Howald, *Rev. Mod. Phys.* **75**, 1201 (2003).
- ⁸ A. N. Lavrov and L. P. Kozeeva, *Physica C* **248**, 365 (1995); **253**, 313 (1995); *JETP Lett.* **62**, 580 (1995).
- ⁹ A. N. Lavrov, M. Yu. Kameneva, and L. P. Kozeeva, *Phys. Rev. Lett.* **81**, 5636 (1998).
- ¹⁰ A. N. Lavrov, Y. Ando, K. Segawa and J. Takeya, *Phys. Rev. Lett.* **83** (1999) 1419.
- ¹¹ M. Yu. Kameneva, L. P. Kozeeva, A. N. Lavrov, E. V. Sokol, and V. E. Fedorov, *J. Cryst. Growth* **231**, 171 (2001).
- ¹² A pronounced crossover was reproducibly observed in the *c*-axis resistivity of underdoped $R\text{Ba}_2\text{Cu}_3\text{O}_{6+x}$ crystals^{8,9,10,11} and some other layered oxides²⁶, yet its origin is still insufficiently understood.
- ¹³ J. H. Brewer *et al.*, *Phys. Rev. Lett.* **60**, 1073 (1988).
- ¹⁴ S. Sanna, G. Allodi, G. Concas, A. D. Hillier, and R. De Renzi, *Phys. Rev. Lett.* **93**, 207001 (2004).
- ¹⁵ M. R. Trunin, *Phys. Usp.* **48**, 979 (2005).
- ¹⁶ A. Aharony, R. J. Birgeneau, A. Coniglio, M. A. Kastner, and H. E. Stanley, *Phys. Rev. Lett.* **60**, 1330 (1988).
- ¹⁷ E. L. Nagaev, *Phys. Usp.* **38**, 497 (1995).
- ¹⁸ C. Timm and K. H. Bennemann, *Phys. Rev. Lett.* **84**, 4994 (2000).
- ¹⁹ O. P. Sushkov and V. K. Kotov, *Phys. Rev. B* **70**, 024503 (2004).
- ²⁰ V. Juricic, M. B. Silva Neto, and C. Morais Smith, *Phys. Rev. Lett.* **96**, 077004 (2006).
- ²¹ R. J. Gooding, N. M. Salem, R. J. Birgeneau, and F. C. Chou, *Phys. Rev. B* **55**, 6360 (1997).
- ²² V. F. Gantmakher, L. P. Kozeeva, A. N. Lavrov, D. A. Pushin, D. V. Shovkun, G. E. Tsydynzhapov, *JETP Lett.* **65**, 870 (1997).
- ²³ X. F. Sun, K. Segawa, and Y. Ando, *Phys. Rev. B* **72**, 100502 (2005).
- ²⁴ In a strict sense MIT is determined only at $T = 0$. However, if the state of the electronic system changes with temperature, one can introduce an effective MIT temperature, T_{MIT} , so that the states “quenched” from $T > T_{\text{MIT}}$ and $T < T_{\text{MIT}}$ would correspond to a metal and an insulator at $T = 0$.
- ²⁵ D. P. Arovas, A. J. Berlinsky, C. Kallin, and S.-C. Zhang, *Phys. Rev. Lett.* **79**, 2871 (1997).
- ²⁶ T. Valla, P. D. Johnson, Z. Yusof, B. Wells, Q. Li, S. M. Loureiro, R. J. Cava, M. Mikami, Y. Mori, M. Yoshimura, and T. Sasaki, *Nature (London)* **417**, 627 (2002).